Binding Kinetics and SWNT Bundle Dissociation in Low Concentration Polymer−Nanotube Dispersions

Jonathan N. Coleman,* Alexander Fleming, Stefanie Maier, Sean O'Flaherty, Andrew I. Minett, Mauro S. Ferreira, Stefan Hutzler, and Werner J. Blau

Department of Physics, Trinity College Dublin, Dublin 2, Ireland

Received: September 5, 2003; In Final Form: January 5, 2004

Single-wall carbon nanotubes are severely restricted by the fact that they exist in bundles. In addition, their interaction with other materials is poorly understood. In this work a new spectroscopic method is described to measure the ratio of free polymer to nanotube-bound polymer in SWNT/polymer solutions. This ratio is highly nonlinear and can be described by a model based on polymer−nanotube adsorption/desorption kinetics. In combination with the experimental data, this model shows that the nanotube bundles decrease in size as the concentration is reduced. Individual nanotubes are stable at low concentration, as supported by atomic force microscopy data. In addition, the model allows the indirect measurement of the polymer−nanotube binding energy at 1.1 eV per molecule. In principle, this method is generic and can be used to monitor dispersions of any metallic nanomaterials in suitable, luminescent organic solutions.

1. Introduction

Single-wall nanotubes (SWNT) have generated much interest in recent years due to their unique properties and huge potential for applications.[1] However, some fundamental problems remain to be addressed. Not least is the fact that SWNT are almost always present in the form of bundles. These bundles can be quite large with diameters of tens of nanometers and lengths of many micrometers. In addition they tend to have properties distinctly inferior to those of individual nanotubes.

Therefore in most areas of nanotube research it would be advantageous to have access to samples of dispersed individual nanotubes. Failing that, it would be desirable, at the very least, to have some control over the bundle size. This is the case not only for fundamental studies where individual SWNT are essential but for more applied studies such as composite research where uniform dispersions are required. Examples of this include electrical percolation studies where the presence of bundles increases the percolation threshold[2] and mechanical reinforcement where shear slippage in bundles reduces the effectiveness of SWNT as reinforcement agents.[3] While it is possible to obtain individual nanotubes by dispersion of SWNT in surfactants followed by ultra-centrifugation, this is a very inefficient method with >99% of SWNT being lost from the dispersion.[4]

In addition, much work has been published recently on properties of polymer−nanotube composites.[5−7] However, to date, understanding of the polymer−nanotube interactions, the binding scheme, and the magnitude of the polymer−nanotube binding energy remains poor. This results in very little being understood about the role of polymer−nanotube kinetics in composite formation.

In this work we aim to address these problems by the introduction of a new spectroscopic method to study polymer−nanotube adsorption/desorption kinetics. This method allows the measurement of the fraction of unbound polymer as a function of concentration in polymer−nanotube solutions. Using a simple model based on adsorption/desorption equilibrium, we can then calculate the polymer−nanotube binding energy. In addition, the data show that bundles spontaneously break up as the solution concentration is reduced until predominately individual SWNT are observed at low concentrations.

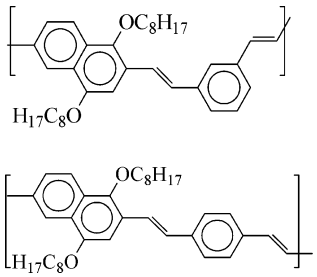

Figure 1. Molecular structure of the polymers used in this study; top: mpNV, bottom: ppNV.

2. Sample Preparation and Experimental Method

The purified nanotubes used in this work were prepared by the Hipco process,[8] supplied by Carbon Nanotechnologies Inc. and used without further treatment. The materials used were short chain polymers (see Figure 1), poly[*p*-phenylenevinylene-*co*-(1,5-dioctyloxy-2,6-naphthylene vinylene)] (6 units average, $M_w/M_n \sim 2$), (ppNV) and poly[*m*-phenylenevinylene-*co*-(1,5-dioctyloxy-2,6-naphthylene vinylene)](12 units average, $M_w/M_n \sim 4$), (pmNV) and were synthesized in house.[9] Two identical solutions of each polymer in chloroform were made with concentration approximately 1.7×10^{-2} kg/m^3 (kg/m^3 = g/L = mg/mL). To one solution of each polymer was added pure Hipco SWNT such that the polymer−SWNT mass ratio was 1:1. All four solutions were then initially diluted by a factor of 2 with pure chloroform. This was then repeated ∼20 times to give 20 sets of concentrations (dilution factor = 2/3 at lower concentrations), each with two polymer solutions (ppNV and pmNV) and two polymer/SWNT composite solutions. This results in a concentration range of 1.7×10^{-2} kg/m^3 to ∼1.8 ×

* Author to whom correspondence should be addressed. Tel: ++35316083859. E-mail: colemaj@tcd.ie.

10.1021/jp036651+ CCC: $27.50
Published on Web 02/20/2004

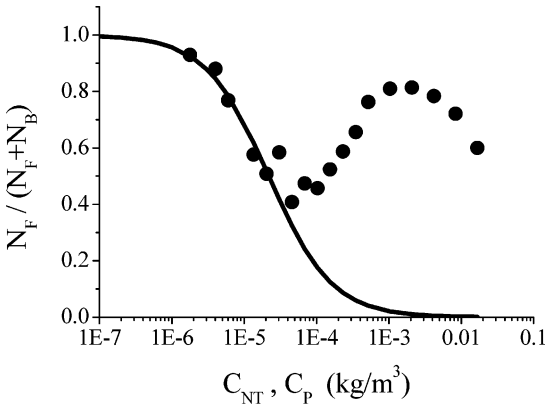

Figure 2. Graph of the fraction of free polymer as a function of concentration for mpNV, where N_F and N_B are the number of free and bound polymer molecules, respectively. The fraction of free polymer was calculated from the ratio of the photoluminescence intensity for a composite solution to the photoluminescence intensity for the equivalent polymer solution. Note that for all concentrations the partial nanotube concentration, C_{NT}, equals the partial polymer concentration, C_P. The solid line is a fit to eq 7a in the low concentration regime.

10^{-6} kg/m^3. It should be noted that for each concentration, the partial polymer concentration of the polymer/SWNT solution is the same as the polymer concentration in the equivalent polymer solution. In addition, for each composite solution, at every concentration the partial nanotube concentration is equal to the partial polymer concentration. Each solution was sonicated for 20 s using a high power sonic tip and then allowed to stand for 24 h to come to equilibrium. No sedimentation was observed over this period. It should be noted at this point that unfunctionalized SWNT such as those used here cannot be effectively dispersed in chloroform. Mixing of SWNT and chloroform in the absence of polymer results in the aggregation and sedimentation of the nanotube material within minutes.

Photoluminescence measurements were carried out using an LS-55 Perkin-Elmer luminescence spectrometer with an excitation wavelength of 400 nm. Atomic force microscopy (AFM) measurements were performed using a Digital Instruments Nanoscope IIIA Microscope operating in tapping mode. Samples for AFM were prepared by soaking amino-silanized pre-cleaned SiO_2 wafers in composite solutions for 5−7 days.

3. Results and Discussion

Photoluminescence (PL) measurements were performed on all polymer and polymer/SWNT solutions. For each concentration, the integrated PL was lower in the polymer/SWNT solution compared to the equivalent polymer solution. In the case of the polymer/SWNT solutions, the polymer molecules exist in two forms, free polymer and polymer that is bound to the SWNT. For bound polymer chains, the PL efficiency is expected to be extremely low as any photogenerated singlet excitons preferentially decay nonradiatively through the fast vibrational manifold of the nanotubes.[10] Thus any observed PL from the polymer/SWNT solutions is due to the free polymer only. This means that the ratio of PL intensity for a polymer/SWNT solution to that of a polymer solution of equivalent concentration is a measure of the fraction of free polymer molecules in the composite solution at that concentration.

For all concentrations, the fraction of free polymer was calculated from the intensity ratio and is plotted in Figure 2. Due to constant polymer adsorption/desorption from the nanotubes, this fraction of free polymer is not expected to be constant over the concentration range studied. Indeed this plot is highly nonlinear with concentration; however, it approaches 1 at very low concentrations, indicating that most molecules are unbound at low concentration.

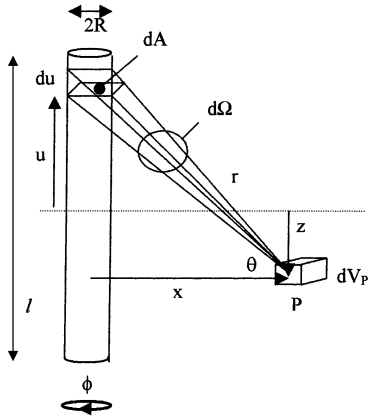

Figure 3. Geometry used to derive equation for absorption rate. Note that x, ϕ, and z are cylindrical polar coordinates, u is the position along the cylinder. The volume of the box at P is $dV_P = xdxdzd\phi$. V_P is at a distance r from P to the point on the cylinder, u. The angle between r and x is θ, while the solid angle defined by dA about P is dΩ. The cylinder has a diameter $2R$ and a length l.

To understand this experimental data, a model is required to describe the polymer−SWNT adsorption−desorption kinetics as a function of concentration. When the system is in equilibrium at a given concentration, the adsorption rate will equal the desorption rate. For an arbitrary concentration, the adsorption rate can be calculated as follows.

Consider an isolated cylinder of diameter $2R$ and length l in a polymer solution as shown in Figure 3. This cylinder can be thought to represent a bundle of nanotubes. In addition, consider a small volume of space at point P, dV_P. The polymer molecules originally in dV_P undergo diffusion with a finite probability that a given molecule will arrive at the bundle between the positions u and $u + du$. We assume that any molecule that reaches the bundle adsorbs through a van der Waals interaction. The probability for adsorption, $d\Pi$, is given by the solid angle $d\Omega$, spanning the area dA, centered on P. Thus the fraction of molecules originally in dV_P that arrive and adsorb at dA is given by

$$d\Pi = \frac{d\Omega}{4\pi} = \frac{2Rdu\cos\theta}{4\pi r^2} = \frac{Rxdu}{2\pi r^3} \tag{1}$$

The time taken, on average, for a polymer molecule to travel a distance r, from P to dA can be calculated statistically in terms of a random walk and is given by

$$r^2 = \frac{16D}{\pi}t \tag{2}$$

where D is the diffusion coefficient for the polymer molecules.[11] The probability rate for molecules traveling from P to dA is $d\Pi/dt$:

$$\frac{d\Pi}{dt} = \frac{d\Pi}{dr}\frac{dr}{dt} = \frac{-12DRxdu}{\pi^2(x^2+(u-z)^2)^{5/2}} \tag{3}$$

where

$$r = \sqrt{x^2+(u-z)^2}$$

Multiplying eq 3 by N_P, the number of molecules originally in dV_P and integrating over the length of the bundle u and over

the volume of solution occupied by the bundle then gives the adsorption rate. Note, $N_P = (N_F/V)dV_P = (N_F/V)xdxdzd\phi$. Here (N_F/V) is the number of free molecules per unit volume and $dV_P = xdxdzd\phi$ in cylindrical polar coordinates. This gives the adsorption rate $(-dN/dt)$ as

$$-\frac{dN}{dt} = \frac{24DR}{\pi}\frac{N_F}{V}\int_{z=-A}^{z=A}\int_{x=R}^{x=A}\int_{u=-l/2}^{u=l/2}\frac{x^2dxdudz}{(x^2+(u-z)^2)^{5/2}} = \frac{24DR}{\pi}\frac{N_F}{V}f \quad (4)$$

where f is the value of the triple integral and A is the spatial extent of the volume of solution per bundle; $V_{bun} = 2\pi A^3$. This volume is modeled as a cylinder of radius A and height 2A and is related to the concentration by $V_{bun} = m_{bun}/C_{NT}$ (see below). It should be noted at this point that this model assumes a sticking probability of 1 and is only valid in the limit of low polymer coverage. If in reality the sticking probability is less than 1, this means that we will have overestimated the adsorption rate. As will become apparent, this will result in an underestimation of the binding energy.

For extended polymer molecules on graphite surfaces, desorption has been shown to follow first-order kinetics.[12] This means we can write down the desorption rate $(-dN/dt)$ as

$$-\frac{dN}{dt} = \nu\left[\frac{N_B}{V}V_{bun}\right]e^{-E_B/kT} \quad (5)$$

where ν is a preexponential frequency factor, E_B is the polymer−nanotube binding energy, N_B/V is the number of bound molecules per unit volume and V_{bun} is the volume of solution occupied by one bundle. This latter parameter is defined by the nanotube concentration, C_{NT}, and can be found from

$$C_{NT} = \frac{N_{bun}m_{bun}}{V}$$

where N_{bun}/V is the number of bundles per unit volume and m_{bun} is the bundle mass. This allows the volume of solution per bundle to be calculated as

$$V_{bun} = \frac{V}{N_{bun}} = \frac{m_{bun}}{C_{NT}}$$

Substituting this into eq 5 gives the desorption rate

$$-\frac{dN}{dt} = \nu\frac{N_B}{V}\frac{m_{bun}}{C_{NT}}e^{-E_B/kT} \quad (6)$$

At equilibrium, the adsorption rate equals the desorption rate, so by equating eqs 4 and 6, rearranging, and noting that $m_{bun} = \rho_{bun}\pi R^2 l$, and the bundle surface area, $A_{bun} = 2\pi Rl$, we get

$$\frac{N_F}{N_F+N_B} = \frac{1}{1+C_{NT}/C_0} \quad (7a)$$

with

$$C_0 = \frac{\pi^2\nu\rho_{bun}A_{bun}e^{-E_B/kT}}{48Df} \quad (7b)$$

where C_0 is a characteristic concentration, ρ_{bun} is the bundle mass density, N_F is the number of free molecules, N_B is the number of bound molecules, and so $N_F/(N_F+N_B)$ is the fraction of free polymer.

Thus the fraction of free polymer at a given concentration is controlled by the diffusion coefficient D, a space integral f, the desorption preexponential frequency factor ν, the bundle mass density ρ_{bun}, the bundle surface area A_{bun}, the polymer−nanotube binding energy E_B, and the absolute temperature T. All of these factors are known or can be estimated except the bundle surface area and the binding energy. The diffusion coefficient, D, can be found from the Stokes−Einstein equation:[11]

$$D = \frac{kT}{6\pi\eta a} \quad (8)$$

where η is the viscosity and a is the polymer hydrodynamic radius. For low concentration solutions, the viscosity is very close to the solvent viscosity giving $\eta \approx \eta_{chloroform} = 0.536 \times 10^{-3}$ s Pa. The hydrodynamic radius can be estimated from the polymer density and the mass of the polymer molecule as measured by chromatography. In both cases the density is 1.3 g/cm^3, while for mpNV, $m = 1.01 \times 10^{-23}$ kg (12 repeat units) while for ppNV, $m = 4.61 \times 10^{-24}$ kg (6 repeat units). This allows calculation of the diffusion coefficient as $D = 3.31 \times 10^{-10}$ m^2/s for mpNV and $D = 4.30 \times 10^{-10}$ m^2/s for ppNV. The spatial integral, f, was calculated numerically and was found to be close to 800 for the entire concentration range studied. The bundle mass density is approximately, $\rho_{bun} = 1.5$ g/cm^3 for Hipco SWNT.[13]

According to transition state theory,[14] the preexponential frequency factor, ν, for first-order desorption is given by

$$\nu = \left(\frac{kT}{h}\right)\frac{q_d}{q_a} \quad (9)$$

where q_d is the partition function for the transition state for desorption and q_a is the partition function for the adsorbed state. The factor (kT/h) has a value of approximately 10^{13} Hz, while the ratio (q_d/q_a) is expected to be large for an extended molecule. Two studies have recently been carried out on desorption of extended molecules from graphite. In one of these papers, desorption of alkanes with a range of chain lengths was measured.[12] In this work a value of $\nu = 10^{19.6}$ Hz was reported. In the other paper, experiments on desorption of acetone were carried out giving $\nu = 10^{20.5}$ Hz.[15] Thus in this work we will assume a value of $\nu = 10^{20}$ Hz for the preexponential frequency factor.

As discussed previously, the fraction of free polymer as a function of concentration in the composite solutions is described by eq 7a. If the characteristic concentration, C_0, were constant, the fraction of free polymer would be expected to decrease monotonically with increasing concentration. From Figure 2, this is clearly not the case. As the polymer−nanotube binding energy is expected to be constant, this suggests that the bundle surface area in fact varies with concentration. This can be tested by transforming the data in Figure 2 to represent C_0 as a function of concentration using eq 7a. These data are presented in Figure 4 (left axis).

These data show that C_0 decreases smoothly as the concentration is decreased before saturating at $C_0 = 2.2 \times 10^{-5}$ kg/m^3 at low concentration. As $C_0 \propto A_{bun}$, this indicates that the bundle surface area decreases as the concentration is decreased before saturating at a minimum value, suggesting that as the concentration is decreased the bundles spontaneously break up. As they reach a minimum size, this indicates that individual nanotubes are stable in solutions below 3×10^{-5} kg/m^3. The solid line in Figure 2 is a plot of eq 7a in this region using the saturation

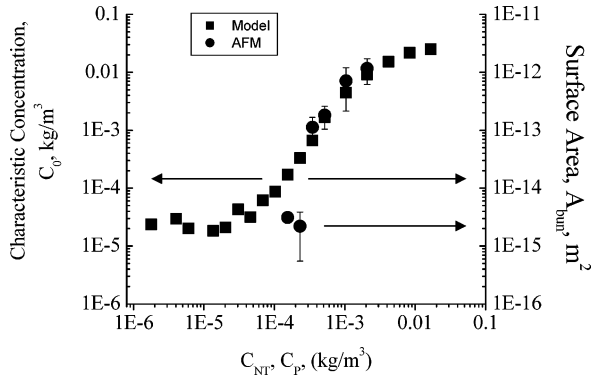

Figure 4. Characteristic concentration as a function of concentration for mpNV (squares, left axis). The decrease in C_0 as the concentration decreases is indicative of debundling. The characteristic concentration can be used to calculate the bundle surface area using eq 7b (right axis). Superimposed on these data are AFM measurements of the bundle surface area at higher concentrations (circles, right axis). Both data sets are in excellent agreement. Note that for all concentrations the partial nanotube concentration, C_{NT}, equals the partial polymer concentration, C_P.

value of $C_0 = 2.2 \times 10^{-5}$ kg/m^3. This clearly shows that this function fits the experimental data extremely well.

If we know that predominately individual nanotubes are found at low concentration, we can use eq 7b to estimate the polymer−nanotube binding energy. Using that saturation value for C_0 and taking average SWNT dimensions as measured by AFM of diameter = 0.9 nm and length = 750 nm, we can calculate that $E_B = 1.10$ eV per molecule = 106 kJ/mol for pmNV and $E_B = 1.08$ eV per molecule = 104 kJ/mol for ppNV. These values are equivalent within error. However, as described previously, the chain lengths for these molecules are significantly different with approximately 12 and 6 repeat units for pmNV and ppNV, respectively. This indicates that these molecules are not binding to the nanotube over their entire length but that only a section of each is attached.

This is in fact reasonable. Recently, in het Panhuis et al.[16] have carried out ab-initio calculations on the interactions of a conjugated polymer with a SWNT. In this case the polymer PmPV is very similar to the polymers used here. The polymer−nanotube binding energy was calculated as approximately 80 meV per polymer carbon atom. This is in good agreement with Paserba et al. who calculated a binding energy of alkanes on graphite as 75 meV per alkane carbon atom.[12] Other studies have found 64 meV per C atom for alkanes desorbing from Au(111),[17] 140 meV per C atom for alkanes desorbing from silicalite crystals, and 48 meV per C atom for linear alcohols desorbing from Ag(110).[18] If we assume that in our case the binding energy per carbon is 80meV, this means that only about 13−14 carbon atoms are binding per molecule. While this number is relatively low, it should be noted that the spatial extent of 14 C atoms in the polymers studied here is approximately 0.85 nm, similar to the diameter of the nanotubes. This suggests that the polymer molecules do not wrap around the SWNT as has been suggested previously.[19−21] This is not surprising given that the elastic energy cost to the polymer would be high for such high curvature binding. However, this relatively low value for the total number of bound C atoms may be in part due to an overestimation of the sticking probability as mentioned above. However this effect is expected to be minimal.

Using eq 7b, it is possible to transform the data for C_0 shown in Figure 4 into a graph of average bundle surface area as a function of concentration. This is presented in Figure 4 (right axis) and clearly shows that the bundle surface area decreases by 3 orders of magnitude between 1.7×10^{-2} kg/m^3 and ~3 ×

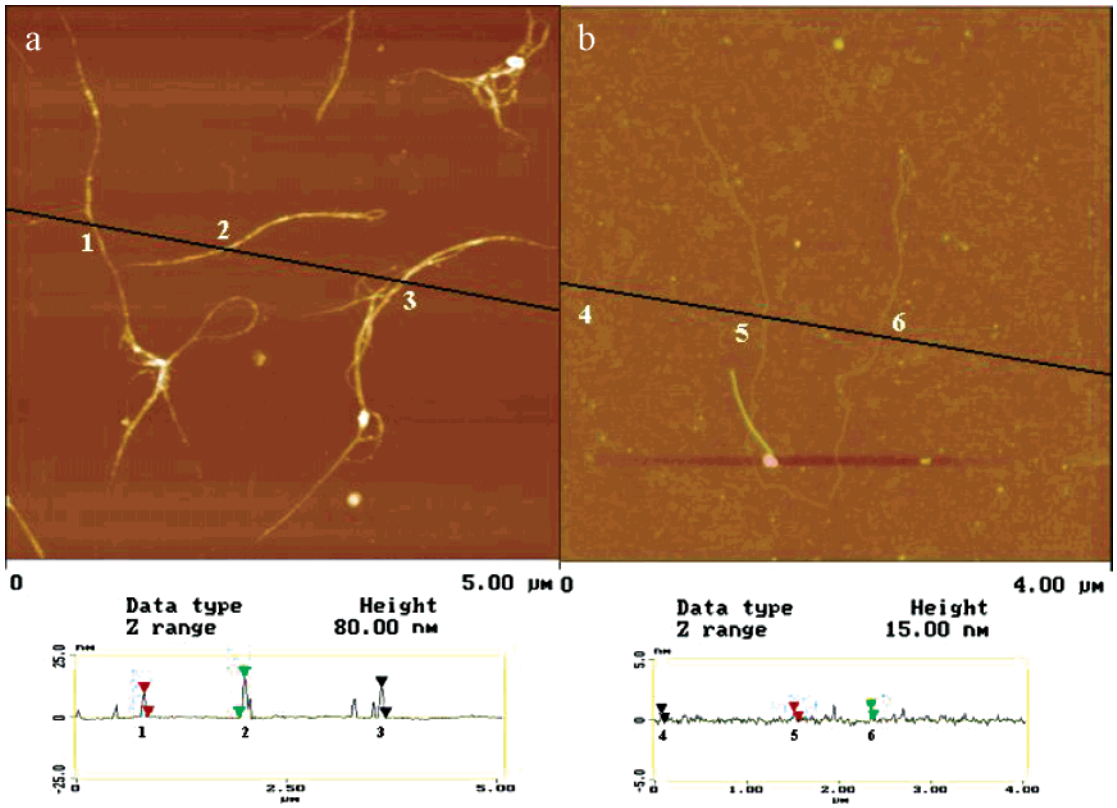

Figure 5. Tapping mode atomic force microscopy images of adsorbed bundles/nanotubes on SiO_2 from (a) $C = 5.2 \times 10^{-4}$ kg/m, with bundles only and (b) $C = 2.3 \times 10^{-4}$ kg/m^3 with predominately SWNT. Note that in (a) the bundles are already dissociating. Below are corresponding height profiles indicating: 1: 9.7 nm, 2: 16.3 nm, 3: 12.5 nm, 4: 0.72 nm, 5: 0.77 nm, 6: 0.90 nm.

10^{-5} kg/m^3. This phenomenon means it is possible to select SWNT bundle area, and hence size, in any composite solution by dilution to the required concentration. Knowledge of the surface area of the bundles as a function of concentration allows the calculation of many other parameters such as the number of nanotubes per bundle as a function of concentration. One of these parameters is the number of bound polymer molecules per nanotube/bundle. At low concentration this is as low as 10 molecules per nanotube. This justifies the original assumption of low polymer coverage at low concentration.

To verify the bundle surface areas predicted by the model and fraction of free polymer measurements, AFM measurements were carried out on bundles extracted from the composite solutions over a range of concentrations between 2.1×10^{-3} kg/m^3 and 1.5×10^{-4} kg/m^3. For the highest concentration sample, very large bundles with diameters of 35−50 nm and lengths of 5−10 μm were observed. In general, as the concentration is decreased, both the length and diameter fall monotonically. The aspect ratio, however, increases with decreasing concentration, suggesting that nanotubes or small bundles of nanotubes detach from the bundle surface. AFM images of the 5.2×10^{-4} kg/m^3 and 2.3×10^{-4} kg/m^3 concentrations are shown in Figure 5. It is clear from these images that the bundles are beginning to unravel at the higher concentration. This is consistent with the increase in aspect ratio. However, for the lowest concentration, mainly isolated SWNT were observed (diameter, 0.7−1 nm; average length, 750 nm; see Figure 5b) with only one bundle seen.

For each concentration, the average surface area was found by measuring the length and diameters for between three and thirty bundles, depending on the concentration. These data are also shown in Figure 4 (right axis) and for the most part agree very well with the original curve. It is not clear why mainly SWNT were observed in the $C = 2.3 \times 10^{-4}$ kg/m^3 sample. However, the extent of the agreement is strong evidence that both the spectroscopic measurement of the fraction of free polymer and the model presented are reliable.

It is important to point out that the polymer acts not just as a probe but also plays a central role in the dispersion of the nanotubes. It has already been noted that SWNT cannot be dispersed in chloroform in the absence of a suitable polymer. This strongly suggests that the binding energy per unit area between the polymer and SWNT is greater that that between the solvent and the nanotubes. Thus the bundle size at a given concentration is most likely controlled by a trade-off between the bundle−polymer surface energy and the bulk cohesive energy of the bundle. Further studies are underway to understand this phenomenon in detail.

4. Conclusion

In conclusion, a novel spectroscopic method has been introduced to measure the fraction of free molecules in a luminescent polymer−SWNT solution. This shows that the fraction of free polymer is highly nonlinear, indicating the presence of complex adsorption/desorption kinetics. To explain this, a simple model based on adsorption/desorption equilibrium was introduced. The model indicates that the fraction of free polymer is critically dependent on the polymer−nanotube binding energy and the surface area of the nanotube bundles. The model can be used in conjunction with the data to generate a plot of bundle surface area as a function of concentration. These data suggests that the bundles break up as the concentration is lowered until isolated SWNT are stable at low concentrations. This is supported by AFM data. Thus this represents a new method for the controlled debundling of SWNT. In addition, the stability of isolated nanotubes at low concentration allows an indirect measurement of the polymer−nanotube binding energy. In principle this method can be used to monitor dispersions of any metallic nanomaterials in suitable, luminescent organic solutions.

Acknowledgment. The authors acknowledge financial support from the Irish Higher Education Authority, Enterprise Ireland, and the European Union.

References and Notes

(1) Baughman, R. H.; Zakhidov, A. A.; de Heer, W. A. *Science* **2002**, *297*, 787.
(2) Munson-McGee, S. H. *Phys. Rev. B* **1991**, *43*, 3331.
(3) Cadek, M.; Coleman, J. N.; Ryan, K. P.; Nicolosi, V.; Bister, G.; Fonseca, A.; Nagy, J. B.; Szostak, K.; Béguin, F.; Blau, W. J. *Nano Letters* **2004**, *4*, 353.
(4) O'Connell, M. J.; Bachilo, S. M.; Huffman, C. B.; Moore, V. C.; Strano, M. S.; Haroz, E. H.; Rialon, K. L.; Boul, P. J.; Noon, W. H.; Kittrell, C.; Ma, J. P.; Hauge, R. H.; Weisman, R. B.; Smalley, R. E. *Science* **2002**, *297*, 593.
(5) Dalton, A. B.; Collins, S.; Muñoz, E.; Razal, J. M.; Ebron, V. H.; Ferraris, J. P.; Coleman, J. N.; Kim, B. G.; Baughman R. H. *Nature* **2003**, *423*, 703.
(6) Cadek, M.; Coleman, J. N.; Barron, V.; Hedicke, K.; Blau, W. J. *Appl. Phys. Lett.* **2002**, *81*, 5123.
(7) Coleman, J. N.; O'Brien, D. F.; Dalton, A. B.; McCarthy, B.; Lahr, B.; Drury, A.; Barklie, R. C.; Blau, W. J. *Chem. Commun.* **2000**, *20*, 2000.
(8) Nikolaev, P.; Bronikowski, M. J.; Bradley, R. K.; Rohmund, F.; Colbert, D. T.; Smith, K. A.; Smalley, R. E. *Chem. Phys. Lett.* **1999**, *313*, 91.
(9) Maier, S. et al. In preparation
(10) Ago, H.; Shaffer, M. S. P.; Ginger, D. S.; Windle, A. H.; Friend, R. H. *Phys. Rev. B* **2000**, *61*, 2286. Wery, J.; Aarab, H.; Lefrant, S.; Faulques, E.; Mulazzi, E.; Perego, R. *Phys. Rev. B* **2003**, *67*, 115202.
(11) Atkins, P. W. *Physical Chemistry*; Oxford University Press: Oxford, 1992.
(12) Paserba, K. R.; Gellman A. J. *J. Chem. Phys.* **2001**, *115*, 6737.
(13) Coleman, J. N.; Blau, W. J.; Dalton, A. B.; Muñoz, E.; Collins, S.; Kim, B. G.; Razal, J.; Selvidge, M.; Vieiro, G.; Baughman, R. H. *Appl. Phys. Lett.* **2003**, *82*, 1682.
(14) Zhdanov, V. P. *Surf. Sci. Rep.* **1991**, *12*, 183.
(15) Kwon, S.; Vidic, R.; Borguet, E. *Surf. Sci.* **2003**, *522*, 17.
(16) in het Panhuis, M.; Maiti, A.; Dalton, A. B.; van den Noort, A.; Coleman, J. N.; McCarthy, B.; Blau, W. J. *J. Phys. Chem. B* **2003**, *109*, 478.
(17) Wetterer, S. M.; Lavrich, D. J.; Cummins, T.; Bernasek, S. L.; Scoles, G. *J. Phys. Chem. B* **1998**, *102*, 9266.
(18) Zhang, R.; Gellman, A. J. *J. Phys. Chem.* **1991**, *95*, 7433.
(19) McCarthy, B.; Coleman, J. N.; Czerw, R.; Dalton, A. B.; in het Panhuis, M.; Maiti, A.; Drury, A.; Bernier, P.; Nagy, J. B.; Lahr, B.; Byrne, H. J.; Carroll, D. L.; Blau, W. J. *J. Phys. Chem. B* **2002**, *106*, 3087.
(20) Star, A.; Liu, Y.; Grant, K.; Ridvan, L.; Stoddart, J. F.; Steuerman, D. W.; Diehl, M. R.; Boukai, A.; Heath, J. R. *Macromolecules* **2003**, *36*, 553.
(21) O'Connell, M. J.; Boul, P.; Ericson, L. M.; Huffman, C.; Wang, Y. H.; Haroz, E.; Kuper, C.; Tour, J.; Ausman, K. D.; Smalley, R. E. *Chem. Phys. Lett.* **2001**, *342*, 265.